DRIFT COMPRESSION AND FINAL FOCUS OPTIONS FOR HEAVY ION FUSION

Hong Qin[1], Ronald C. Davidson[1], John J. Barnard[2] and Edward P. Lee[3]

1 Plasma Physics Laboratory, Princeton University
2 Lawrence Livermore National Laboratory
3 Lawrence Berkeley National Laboratory

Presented at the 15th Heavy Ion Fusion Symposium

Princeton, NJ, June 7-11, 2004

—Heavy Ion Fusion Virtual National Laboratory —

*Research supported by the U.S. Department of Energy.

Motivation

- In the currently envisioned configurations for heavy ion fusion (HIF), it is necessary to longitudinally compress the beam bunches by a large factor after the acceleration phase and before the beam particles are focused onto the fusion target.
  - In order to obtain enough fusion energy gain, the peak current for each beam is required to be order 10^3A, and the bunch length to be as short as 0.5m.
  - To deliver the beam particles at the required energy, it is both expensive and technically difficult to accelerate short bunches at high current.
- The objective of drift compression is to compress a long beam bunch by imposing a negative longitudinal velocity tilt over the length of the beam in the beam frame.

Drift Compression and Final Focus of Heavy Ion Beam

- Assume a Cs^+ beam for HIF driver with $A = 132.9,\ q = 1,\ (\gamma - 1)mc^2 = 2.43GeV,\ z_{bf} = 0.27$m, and $< I >= 2254$A.

- The goal of drift compression is:
  - Length $z_b \longrightarrow \times\frac{1}{21.8}$. Perveance $K \longrightarrow \times 21.8$.

- Allowable changes of other system parameters:
  - Velocity tilt $|v_{zb}| \longrightarrow \leq 0.01$.
  - Beam radius $a \longrightarrow \times 2.33$.
  - Half lattice period $L \longrightarrow \times\frac{1}{2}$.
  - Filling factor $\eta \longrightarrow \times 4$. $\eta B' \longrightarrow \times 4$.

- The beam pulse need to focused onto a target with 2mm characterisitic size.

Other Presentations at HIF04

- Final focus
  - Th.I-07 **J. Barnard** (LLNL - USA)
- Neturalized final focus
  - W.P-13 **P. Efthimion** (PPPL-USA)
  - W.P-20 **J. Hasegawa** (TiTech-Japan)
  - Th.I-05 **P. Roy** (LBNL - USA)
  - Th.I-06 **D. Welch** (Mission Research Corp - USA)
- Drift compression
  - W.P-19 **W. Sharp** (LLNL-USA)
  - W.P-17 **T. Kikuchi** (Univ. of Tokyo - Japan)
  - Th.I-09 **T. Kikuchi** (Univ. of Tokyo - Japan)

Important Questions

- Longitudinal Dynamics. What is the dynamics of $z_b(s)$?
  - How long is the beam line? ($s_f = 516\text{m}$)
  - How large initial velocity tilt can we afford? ($v_{zb0} = -0.0143$)
  - Stability?
- Transverse Dynamics and Final Focus. How to focus the entire beam onto the target?
  - Non-periodic lattice design, $L(s),\ B'(s),\ \eta(s),\ \kappa(s),\ K(s)$.
  - Non-periodic envelope, matched solutions? adiabatically-matched solutions?

Outline

- Self-similar symmetry if required for focusing the entire beam pulse.
- Longitudinal Dynamics.
  - Self-similar solutions for un-neutralized beams.
  - Self-similar solutions for neutralized beams.
  - Pulse shaping
- Transverse Dynamics and Final Focus.
  - Non-periodic lattice and adiabatically-matched beams.
  - Time-dependent lattice for deviation from self-similar symmetry.

Need Self-Similar Symmetry To Focus the Entire Beam Pulse

- Transverse envelope equations for every slice in a bunched beam,

$$\boxed{\begin{aligned}
\frac{\partial^2 a(s,Z)}{\partial s^2} + \kappa_q(s)a(s,Z) - \frac{2K(s,Z)}{a(s,Z)+b(s,Z)} - \frac{\varepsilon_x^2(s,Z)}{a(s,Z)^3} &= 0,\\
\frac{\partial^2 b(s,Z)}{\partial s^2} - \kappa_q(s)b(s,Z) - \frac{2K(s,Z)}{a(s,Z)+b(s,Z)} - \frac{\varepsilon_y^2(s,Z)}{b(s,Z)^3} &= 0,
\end{aligned}}$$

  - $K(s,Z) \equiv 2e^2\lambda(s,Z)/m\gamma^3\beta^2c^2$ — effective perveance of slice Z.
  - Z — longitudinal coordinate for different slices.
  - $K(s,Z)$ and $\lambda(s,Z)$ are determined by the longitudinal dynamics.

- A lattice design for one slice may not be able to transversely confine other beam slices and focus them onto the same focal spot at the target.

- Most of the other slices cannot be focused at all due to the mismatch induced by the different s-dependences of the current and emittance.

- A fixed drift compression and final focus lattice will be able to focus the entire beam pulse onto the same focal spot only if the current and emittance of all the slices depend on s in the same manner.

Need Self-Similar Symmetry To Focus the Entire Beam Pulse

- a, b, λ, ε_x, and ε_y for different Z are generated by the same solution through a one-parameter group transformation admitted by the envelope equations

$$\begin{pmatrix} a\left[s, Z(\delta=0)\right] \\ b\left[s, Z(\delta=0)\right] \\ \lambda\left[s, Z(\delta=0)\right] \\ \varepsilon_x\left[s, Z(\delta=0)\right] \\ \varepsilon_y\left[s, Z(\delta=0)\right] \end{pmatrix} \longrightarrow \begin{pmatrix} a\left[s, Z(\delta)\right] \\ b\left[s, Z(\delta)\right] \\ \lambda\left[s, Z(\delta)\right] \\ \varepsilon_x\left[s, Z(\delta)\right] \\ \varepsilon_y\left[s, Z(\delta)\right] \end{pmatrix} .$$

- It is easy to check that the following scaling group is a symmetry group of the envelope equations.

$$\begin{pmatrix} a\left[s, Z(\delta)\right] \\ b\left[s, Z(\delta)\right] \\ \lambda\left[s, Z(\delta)\right] \\ \varepsilon_x\left[s, Z(\delta)\right] \\ \varepsilon_y\left[s, Z(\delta)\right] \end{pmatrix} = \begin{pmatrix} \delta a\left[s, Z(\delta=0)\right] \\ \delta b\left[s, Z(\delta=0)\right] \\ \delta^2\lambda\left[s, Z(\delta=0)\right] \\ \delta^2\varepsilon_x\left[s, Z(\delta=0)\right] \\ \delta^2\varepsilon_y\left[s, Z(\delta=0)\right] \end{pmatrix}$$

Need Self-Similar Symmetry To Focus the Entire Beam Pulse

- ⇨ Obtain a family of matched and focused solutions for different slices from that of one slice.
- ⇨ It is called self-similar symmetry because every field quantity for different slices has the same s-dependence.
- ⇨ The ratio of line density between different slices is s independent,

$$\boxed{\frac{\lambda\left[s, Z(\delta')\right]}{\lambda\left[s, Z(\delta)\right]} = \left(\frac{\delta'}{\delta}\right)^2 .}$$

- ⇨ Because s is conserved by the group transformation, the s-dependence and the Z-dependence of $\lambda(s, Z)$ are separable

$$\boxed{\lambda(s, Z) = \lambda_b(s) h(Z) .}$$

- ⇨ Line density during drift compression is determined by the longitudinal dynamics. Need to find self-similar drift compression solutions in the longitudinal direction.
- ⇨ The functions $\lambda_b(s)$ and $h(Z)$ will be determined from the symmetry groups of the governing equations for the longitudinal dynamics.

Longitudinal Dynamics – 1D fluid model

- One dimensional fluid model in the beam frame for
  - $\lambda(t, z)$: line density,
  - $u_z(t, z)$: longitudinal velocity,
  - $p_z(t, z)$: longitudinal pressure.
- g-factor model for electric field **[Davidson & Startsev, PRSTAB 2004]**.

$$\boxed{\begin{aligned} eE_z &= -\frac{ge^2}{\gamma^2}\frac{\partial\lambda}{\partial z}, \\ g &= 2\ln\frac{r_w}{r_b}. \end{aligned}}$$

- Take g and r_b as constants for present purpose.
- External focusing: $-\kappa_z z$.

PPPL

Longitudinal Dynamics – 1D fluid model

- In the beam frame:

$$
\begin{aligned}
\frac{\partial \lambda}{\partial t} + \frac{\partial}{\partial z}(\lambda u_z) &= 0 \ \text{(continuity)},\\
\frac{\partial u_z}{\partial t} + u_z \frac{\partial u_z}{\partial z} + \frac{e^2 g}{m\gamma^5}\frac{\partial \lambda}{\partial z} + \frac{\kappa_z z}{m\gamma^3} + \frac{r_b^2}{m\gamma^3 \lambda}\frac{\partial p_z}{\partial z} &= 0 \ \text{(momentum)},\\
\frac{\partial p_z}{\partial t} + u_z \frac{\partial p_z}{\partial z} + 3p_z \frac{\partial u_z}{\partial z} &= 0 \ \text{(energy)}.
\end{aligned}
$$

- Nonlinear hyperbolic PDE system
- The energy equation is equivalent to

$$\frac{d}{dt}\left(\frac{p_z}{\lambda^3}\right) = 0.$$

Lie Group Symmetry Analysis

- ⇨ The systematic method for finding similarity solutions (group-invariant solutions) for PDEs is the Lie group symmetry analysis.
- ⇨ Two types of point symmetries can be used.
  - **Classical point symmetry**, which transfers a solution of the PDEs into another solution.
  - **Non-classical point symmetry**, under which a solution is invariant.
- ⇨ The symmetry groups of both types are determined by the corresponding infinitesimal generators.
  - Classical point symmetry: linear and algorithmically solvable dertmining equations. Infinitesimal generators form a Lie algebra.
  - Non-classical point symmetry: nonlinear and non-algorithmically-solvable dertmining equations. No infinitesimal Lie algebra.
- ⇨ Once point symmtries are found, similarity solutions can be derived straightforwardly.

3D Lie Algebra for Self-Similar Symmetry

- The infinitesimal generators of the classical point symmetry for the nonlinear PDE system are found to be a 4D Lie algebra

$$\begin{aligned}
\frac{d\lambda}{d\delta} &= 2k_2\lambda \,, \\
\frac{du_z}{d\delta} &= k_2 u_z + k_4\cos(t\sqrt{\kappa}) + k_3\sin(t\sqrt{\kappa}) \,, \\
\frac{dp_z}{d\delta} &= 4k_2 p_z \,, \\
\frac{dz}{d\delta} &= k_2 z - k_3\cos(t\sqrt{\kappa})/\sqrt{\kappa} + k_4\sin(t\sqrt{\kappa})/\sqrt{\kappa} \,, \\
\frac{dt}{d\delta} &= k_1 \,.
\end{aligned}$$

- For every set of k_i, the PDE system reduces to an ODE system, and there is a similarity solution.
- Self-similar symmetry $\longrightarrow$ t is an invariant of the symmetry group transformation $\longrightarrow k_1 = 0$.
- Self-similar solutions by the classical point symmetry form a 3D vector space.

An Example

- $(k_1, k_2, k_3, k_4) = (0, 0, \sin\alpha, \cos\alpha)$. The reduced ODE system can be easily integrated,

$$\boxed{\begin{aligned} \lambda(t,z) &= \lambda_0 \frac{\cos\alpha}{\cos(\alpha + t\sqrt{\kappa})}\,, \\ u_z(t,z) &= -z\frac{z_b'(t)}{z_b(t)} = -z\sqrt{\kappa}\tan(\alpha + t\sqrt{\kappa})\,, \\ p_z(t,z) &= p_{z0}\frac{\cos^3\alpha}{\cos^3(\alpha + t\sqrt{\kappa})}\,, \\ z_b(t) &= z_{b0}\frac{\cos(\alpha + t\sqrt{\kappa})}{\cos\alpha}\,. \end{aligned}}$$

- Maximum compression ratio is

$$\boxed{\frac{\lambda_f}{\lambda_0} = \frac{\cos\alpha}{\cos(\alpha + t_f\sqrt{\kappa})}.}$$

- Choose appropriate values for κ, α, and t_f for required compression ratio and maximum velocity tilt.

Nonclassical Point Symmetries

- For the non-classical point symmetry group, the determining equations are non-linear and difficult to solve for general solutions.
- Case (1). Infinitesimal generator

$$\boxed{\frac{d}{d\delta}(\lambda, u_z, p_z, t, z) = \left(0, \frac{u_z}{z}, 0, 0, 1\right) .}$$

  - Density — flattop.
  - Pressure — flattop.
  - Velocity tilt — linear.
  - Self-similar solution — the same as the previous example.

Nonclassical Point Symmetries

⇨ Case (2). Infinitesimal generator

$$\boxed{\frac{d}{d\delta}(\lambda, u_z, p_z, t, z) = (0, \frac{u_z}{z}, \frac{2p_z}{z}, 0, 1).}$$

⇨ Invariants of the group transformation (in addition to t) :

$$\begin{aligned} \lambda(t,z) &= \lambda_b(t),\ v_{zb}(t) = -\frac{v_z(t,z)}{\frac{z}{z_b(t)}}, \\ p_{zb}(t) &= \frac{p_z(t,z)}{\frac{z^2}{z_b^2(t)}},\ v_{zb}(t) = -\frac{dz_b(t)}{dt}. \end{aligned}$$

Nonclassical Point Symmetries

⇨ The z-dependence drops out,

$$\boxed{\begin{aligned} z_b\lambda_b &= const. = N_b/2\,, \\ z_b^3 p_{zb} &= const. = W\,. \\ \frac{d^2 z_b}{ds^2} + \frac{\kappa_z}{m\gamma^3\beta^2c^2} z_b + \frac{\varepsilon_l^2}{z_b^3} &= 0\,, \end{aligned}}$$

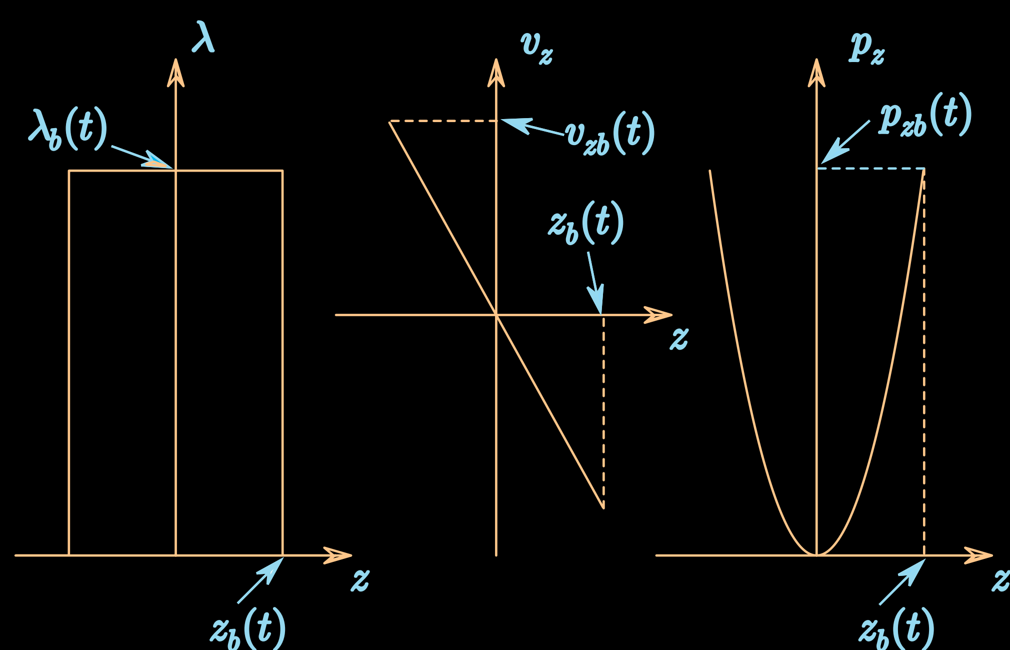

Nonclassical Point Symmetries — Parabolic Self-Similar

⇨ Case (3). Infinitesimal generator

$$\boxed{\frac{d}{d\delta}(\lambda, u_z, p_z, t, z) = (-\frac{2\lambda}{z_b^2(t) - z^2}, \frac{u_z}{z}, -\frac{4p_z}{z_b^2(t) - z^2}, 0, 1).}$$

⇨ Invariants of the group transformation (in addition to t) :

$$\begin{aligned}
\lambda_b(t) &= \frac{\lambda(t,z)}{\left(1 - \frac{z^2}{z_b^2(t)}\right)}, v_{zb}(t) = -\frac{v_z(t,z)}{\frac{z}{z_b(t)}}, \\
p_{zb}(t) &= \frac{p_z(t,z)}{\left(1 - \frac{z^2}{z_b^2(t)}\right)^2}, v_{zb}(t) = -\frac{dz_b(t)}{dt}.
\end{aligned}$$

Nonclassical Point Symmetries — Parabolic Self-Similar

⇨ The z-dependence drops out,

$$\boxed{\begin{aligned} \frac{d\lambda_b}{dt} - \frac{v_{zb}}{z_b}\lambda_b &= 0, \\ \frac{dp_{zb}}{dt} - 3\frac{v_{zb}}{z_b}p_{zb} &= 0. \\ -\frac{dv_{zb}}{dt} - \frac{e^2 g}{m\gamma^5}\frac{2\lambda_b}{z_b} + \frac{\kappa_z z_b}{m\gamma^3} - \frac{4r_b^2 p_{zb}}{m\gamma^3\lambda_b z_b} &= 0\,. \end{aligned}}$$

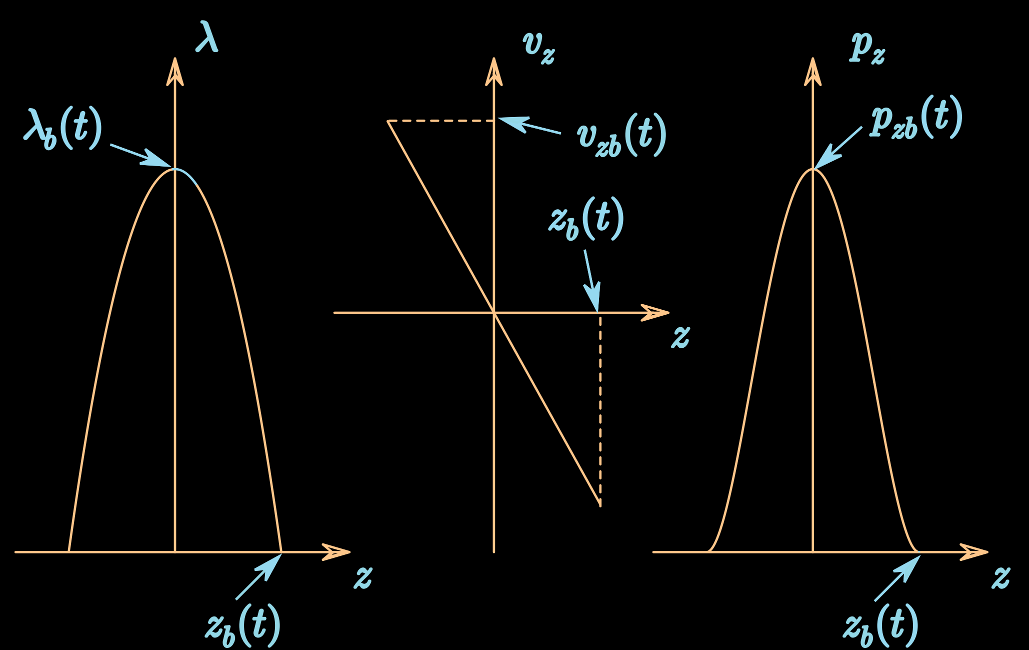

Nonclassical Point Symmetries — Parabolic Self-Similar

⇨ Remarkably, these equations recover the longitudinal envelope equation:

$$\frac{1}{\lambda_b}\frac{d\lambda_b}{dt} + \frac{1}{z_b}\frac{dz_b}{dt} = 0 \Longrightarrow z_b\lambda_b = const. = \frac{3}{4}N_b\,,$$

$$\frac{1}{p_{zb}}\frac{dp_{zb}}{dt} + \frac{3}{z_b}\frac{dz_b}{dt} = 0 \Longrightarrow z_b^3 p_{zb} = const. = W\,,$$

$$\boxed{\frac{d^2 z_b}{ds^2} + \frac{\kappa_z}{m\gamma^3\beta^2c^2}z_b - \frac{K_l}{z_b^2} - \frac{\varepsilon_l^2}{z_b^3} = 0\,,}$$

- $K_l \equiv 3N_b e^2 g/2m\gamma^5\beta^2c^2$ — longitudinal self-field perveance.
- $\varepsilon_l \equiv (4r_b^2 W/m\gamma^3\beta^2c^2N_b)^{1/2}$ — longitudinal emittance.

Nonclassical Point Symmetries — Parabolic Self-Similar

- $\varepsilon_l = 1.0 \times 10^{-5}$ m and $K_z = 2.88 \times 10^{-5}\,\mathrm{m}$, corresponding to an average final current $\langle I_f \rangle = 2254\,\mathrm{A}$, $z_{bf} = 0.268\,\mathrm{m}$, and $g = 0.81$.

- An initial longitudinal focusing force is imposed for $s < 150\,\mathrm{m}$ so that the beam acquires a velocity tilt $z_b' = -0.0143$ at $s_b = 150\,\mathrm{m}$.

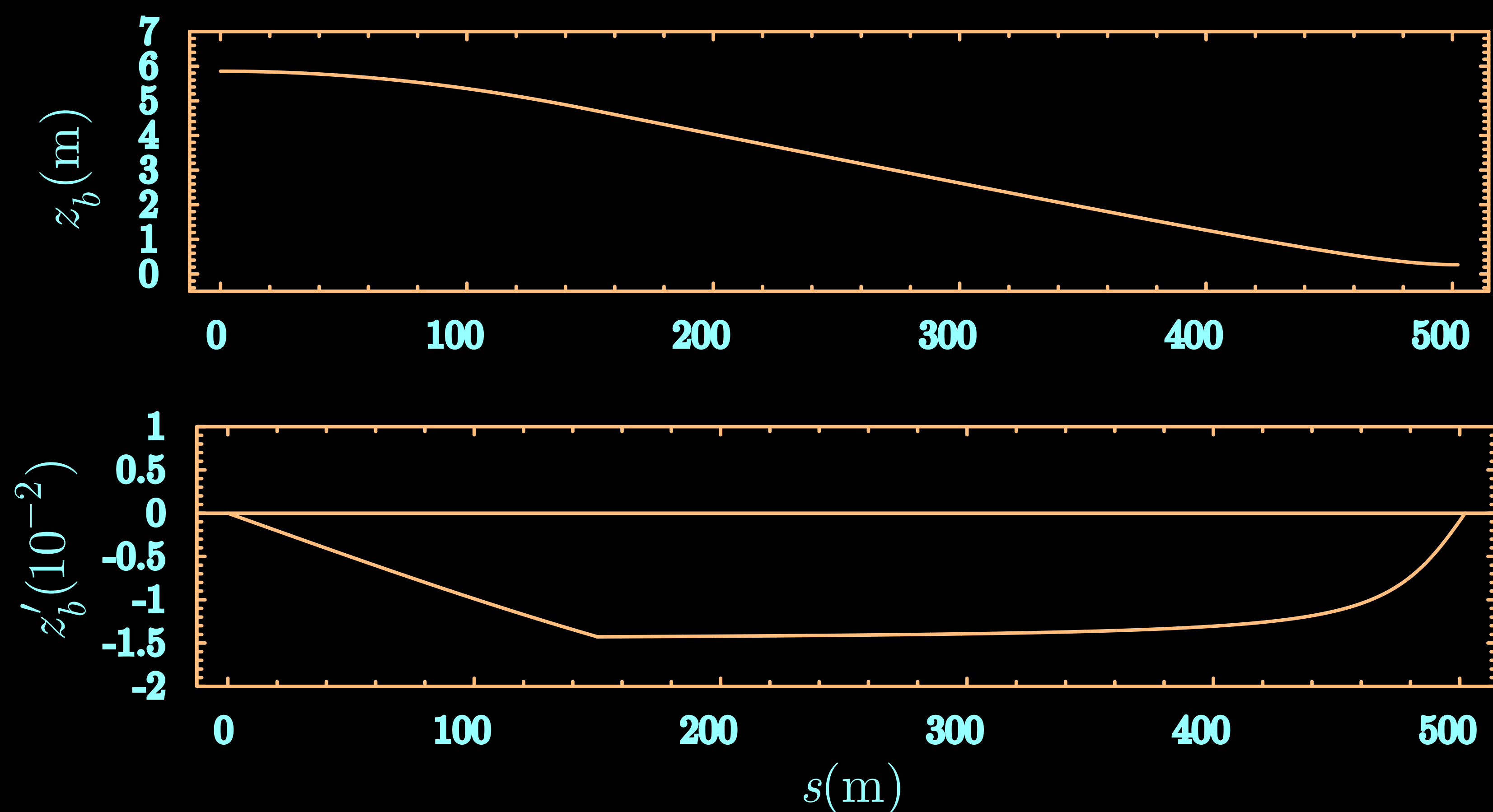

Self-Similar Drift Compression for Neutralized Beams

⇨ Drift compression for neutralized beams modelled by the 1D Vlasov eq.

$$\boxed{\frac{\partial f}{\partial t} + v_z \frac{\partial f}{\partial z} = 0 \,.}$$

⇨ The general solution is a function of two trivial invariants,

$$\boxed{f(t, z, v_z) = f(0, z - v_z t, v_z) \,.}$$

⇨ A class of self-similar drift compression solutions can be more easily constructed using Courant-Snyder invariant

$$\boxed{\begin{aligned} \chi &= \frac{z^2}{z_b^2(t)} + \frac{z_b^2(t)}{z_{b0}^2 v_{T0}^2} \left[v_z - z_b'(t) \frac{z}{z_b(t)} \right]^2 , \\ \frac{d^2 z_b(t)}{dt^2} &= \frac{z_{b0}^2 v_{T0}^2}{z_b^2(t)} \,. \\ z_b^2(t) &= (z_{bo} + z_{b0}' t)^2 + v_{T0}^2 t^2 \,, \end{aligned}}$$

where $z_{b0}' = (dz_b/dt)_{t=0}$ and v_{T0} is an effective thermal speed.

Self-Similar Drift Compression for Neutralized Beams

⇨ Fo the class of distribution $f(\chi)$, the line density is

$$\boxed{\lambda = \int dv_z\ f(\chi) = \frac{z_{b0} v_{T0}}{z_b(t)} \int dV\ f\left[Z^2 + (V - \alpha Z)^2\right] \ ,}$$

where $Z = z/z_b(t)$, $V = z_b v_z/(z_{b0} v_{T0})$, and $\alpha = z_b z_b'/(z_{b0} v_{T0})$.

⇨ $\lambda(t, z)$ has the self-similar form

$$\boxed{\begin{aligned} \lambda(t,z) &= \lambda_b(t) h(Z^2) \ . \\ \lambda_b(t) &= \frac{z_{b0} v_{T0}}{z_b(t)} f_{b0} \ , \quad f_{b0} = \int dV\ f(V^2) \ , \\ h(Z^2) &= \frac{1}{f_{b0}} \int dV\ f\left[Z^2 + (V - \alpha Z)^2\right] \ , \end{aligned}}$$

⇨ The velocity profile is linear,

$$\boxed{u_z = \frac{1}{\lambda} \int dv_z\ v_z f(\chi) = -z_b'(t) Z \ .}$$

Density Inversion Theorem

- For a given self-similar line density profile, the corresponding distribution function is

$$f(\chi) = -\frac{1}{\pi}\frac{\lambda_b(t)z_b(t)}{z_{b0}v_{T0}}\int_\chi^\infty \frac{\partial h(Z^2)}{\partial Z^2}\frac{dZ^2}{\sqrt{Z^2-\chi}} \,.$$

- For the family of self-similar line density profiles

$$\lambda(t,z) = \lambda_b(t)h(Z^2) = \begin{cases} \lambda_b(t)(1-Z^2)^n, & Z \le 1, \\ 0, & Z > 1\,. \end{cases} ,$$

$$f(\chi) = \begin{cases} -\frac{1}{\sqrt{\pi}}\frac{\lambda_b(t)z_b(t)}{z_{b0}v_{T0}}(1-\chi)^{n-1/2}\frac{\Gamma(n)}{\Gamma(n+1/2)}, & \chi \le 1, \\ 0, & \chi > 1\,. \end{cases}$$

  - $n = 1$ and $\lambda \sim 1 - Z^2$,the distribution function $f \sim \sqrt{1-\chi}$ when $\chi \le 1$.
  - $n = 1/2$ and $\lambda \sim \sqrt{1-Z^2}$, f is a flat-top function of χ.
  - $n < 1/2$, the distribution function diverges near $\chi = 1$.

Density Inversion Theorem

⇨ Another family of self-similar line density profiles

$$\lambda(t,z) = \lambda_b(t)h(Z^2) = \begin{cases} \lambda_b(t)(1-Z^{2n}), \ \ Z \le 1, \\ 0, \ Z > 1\,. \end{cases} .$$

$$f(\chi) = \begin{cases} -\frac{1}{\pi}\frac{\lambda_b(t) z_b(t)}{z_{b0} v_{T0}} \Big[\sqrt{\pi} n \chi^{2n-1/2} \frac{\Gamma(1/2-2n)}{\Gamma(1-2n)} \\ + \frac{4n}{4n-1} F(\frac{1}{2}, \frac{1}{2}-2n; \frac{3}{2}-2n; \chi) \Big], \ \ \chi \le 1, \\ 0, \ \chi > 1\,. \end{cases}$$

⇨ $F(\frac{1}{2}, \frac{1}{2}-2n; \frac{3}{2}-2n; \chi)$ —hypergeometric function.

⇨ $2n \gg 1 \longrightarrow$ arbitrarily flat line density profiles.

Longitudinal Pulse Shaping

- The parabolic self-similar drift compression solution requires the initial beam pulse shape to be parabolic.
- Need to shape the beam pulse into a parabolic form before imposing a velocity tilt.
- Need to solve the pulse shaping problem in general — finding the initial velocity distribution $V(z) \equiv v_z(t=0,z)$ such that a given initial pulse shape $\Lambda(z) \equiv \lambda(t=0,z)$ evolves into a given final pulse shape $\Lambda_T(z) \equiv \lambda(t=T,z)$ at time $t=T$.
- Choose the following normalized variables:

$$\overline{v}_z = \frac{v_z}{\beta c}, \ \overline{z} = \frac{z}{z_{b0}}, \ \overline{\lambda} = \frac{\lambda}{\lambda_{b0}}, \ \overline{t} = \frac{t\beta c}{z_{b0}},$$

where z_{b0} is the initial beam half-length, and λ_{b0} is the initial beam line density at the beam center ($z=0$).

Longitudinal Pulse Shaping

⇨ In the normalized variables, the one-dimensional fluid equations, neglecting pressure effects and external focusing, are given by

$$\boxed{\begin{aligned} \frac{\partial \lambda}{\partial t} + \frac{\partial}{\partial z}(\lambda v_z) &= 0 \ \text{(continuity)}, \\ \frac{\partial v_z}{\partial t} + v_z \frac{\partial v_z}{\partial z} + \overline{K}_l \frac{\partial \lambda}{\partial z} &= 0 \ \text{(momentum)}, \end{aligned}}$$

where $\overline{K}_l \equiv \lambda_{b0} e^2 g / m\gamma^5 \beta^2 c^2$ is the normalized longitudinal perveance.

⇨ $\overline{K}_l$ will be treated as a small parameter.

⇨ To order lowest order,

$$\boxed{\begin{aligned} \frac{\partial \lambda}{\partial t} + \frac{\partial}{\partial z}(\lambda v_z) &= 0\,, \\ \frac{\partial v_z}{\partial t} + v_z \frac{\partial v_z}{\partial z} &= 0\,. \end{aligned}}$$

Longitudinal Pulse Shaping

- Can solved by integrating along characteristics. On the characteristics

$$\boxed{\begin{aligned} C \quad : \quad \frac{dz}{dt} &= v_z\,, \\ \frac{d\lambda}{dt} &= -\lambda \frac{\partial v_z}{\partial z}\,, \\ \frac{dv_z}{dt} &= 0\,. \end{aligned}}$$

- Because $dv_z/dt = 0$ on C, the family of characteristics C are straight lines in the (t, z) plan, which can be represented as

$$\boxed{\begin{aligned} C \quad &: \quad z = \xi + V(\xi)t\,, \\ V(\xi) &\equiv v_z(t = 0, \xi)\,. \end{aligned}}$$

Longitudinal Pulse Shaping

- The solution for $v_z(t,z)$ can be formally written as

$$\boxed{v_z(t,z) = V(\xi(t,z))\,,}$$

where $\xi(t,z)$ is a function of t and z.

- From above equations, four useful identities can be derived, *i.e.*,

$$\boxed{\begin{aligned}
\frac{\partial \xi}{\partial z} &= \frac{1}{1+V'(\xi)t}\,, \\
\frac{\partial \xi}{\partial t} &= \frac{-V(\xi)}{1+V'(\xi)t}\,, \\
\frac{\partial v_z}{\partial z} &= \frac{V'(\xi)}{1+V'(\xi)t}\,, \\
\frac{\partial v_z}{\partial t} &= \frac{-V(\xi)V'(\xi)}{1+V'(\xi)t}\,.
\end{aligned}}$$

Longitudinal Pulse Shaping

⇨ We also have

$$\boxed{\frac{d\ln\lambda}{dt} = \frac{-V'(\xi)}{1+V'(\xi)t} \quad \text{on } C\ .}$$

⇨ Since ξ is a constant on C, it can be integrated to give

$$\begin{aligned} \ln\lambda &= \ln\lambda(t=0,\xi) + \int_0^t \frac{-V'(\xi)}{1+V'(\xi)t}dt \\ &= \ln\Lambda(\xi) + \ln[1+V'(\xi)t]\,, \end{aligned}$$

where $\Lambda(z) \equiv \lambda(t=0,z)$ is the initial line density profile. The solution for $\lambda(t,z)$ is

$$\boxed{\lambda(t,z) = \frac{\Lambda(\xi)}{1+V'(\xi)t}\,.}$$

Longitudinal Pulse Shaping

⇨ For the pulse shaping problem, the final line density profile $\Lambda_T(z) \equiv \lambda(t = T, z)$ is specified. We therefore obtain

$$\boxed{\Lambda_T(z) = \Lambda_T[\xi + V(\xi)T] = \frac{\Lambda(\xi)}{1 + V'(\xi)T} ,}$$

which can be viewed as an ordinary differential equation for $V(\xi)$.

⇨ It can be simplified using the variable $U(\xi)$ defined by

$$U(\xi) \equiv \xi + V(\xi)T \, .$$

In terms of $U(\xi)$, $\quad \Lambda_T(U)dU = \Lambda(\xi)d\xi \, .$

⇨ Finally, $U(\xi)$ is determined by solving the above equation for the given functional forms $\Lambda_T(z)$ and $\Lambda(z)$. $V(\xi)$ is simply related to $U(\xi)$ by

$$\boxed{V(\xi) = \frac{U(\xi) - \xi}{T} \, .}$$

Example: Pulse Shaping without Compression

⇨ Consider two examples with the following symmetries and boundary conditions,

$$\begin{aligned} v_z(t,-z) &= -v_z(t,z)\,,\; \lambda(t,-z) = \lambda(t,z)\,, \\ V(\xi &= 0) = 0\,,\; U(\xi = 0) = 0\,. \end{aligned}$$

⇨ **Example 1—Pulse Shaping Without Compression:**

$$\begin{aligned} \Lambda(z) &= \begin{cases} 1 - z^m\,, & 0 \le z \le 1\,, \\ 0\,, & 1 < z\,, \\ \Lambda(-z)\,, & z < 0\,, \end{cases} \\ \Lambda_T(z) &= \begin{cases} (1 - z^n)\dfrac{m(n+1)}{n(m+1)}\,, & 0 \le z \le 1\,, \\ 0\,, & 1 < z\,, \\ \Lambda(-z)\,, & z < 0\,. \end{cases} \end{aligned}$$

Example: Pulse Shaping without Compression

- The equation for U can integrated to give

$$\left[U(\xi) - \frac{U(\xi)^{n+1}}{n+1}\right] \frac{m(n+1)}{n(m+1)} = \xi - \frac{\xi^{m+1}}{m+1} \, .$$

- The parabolic self-similar drift compression solution corresponds to $n = 2$. In this case, there are three solutions for $U(\xi)$. The solution satisfying the right boundary condition is

$$\begin{aligned} U(\xi) &= -\frac{1 - i\sqrt{3} + \sqrt[3]{-2}p^2}{\sqrt[3]{4}p} \, , \\ p &= \sqrt[3]{-3a + \sqrt{-4 + 9a^2}} \, , \\ a &= \frac{2(m+1)}{3m}\left(\xi - \frac{\xi^{m+1}}{m+1}\right) \, . \end{aligned}$$

- For large value of $m \gg 1$, $\Lambda(z)$ has a flat-top shape with a fast fall-off near the ends of the pulse.

Example: Pulse Shaping without Compression

⇨ Initial pulse shape $\Lambda(z) = 1 - z^{15}$ and final pulse shape $\Lambda_T(z) = (45/32)(1 - z^2)$ are plotted in (a). The initial velocity $V(z)$ is plotted in (b).

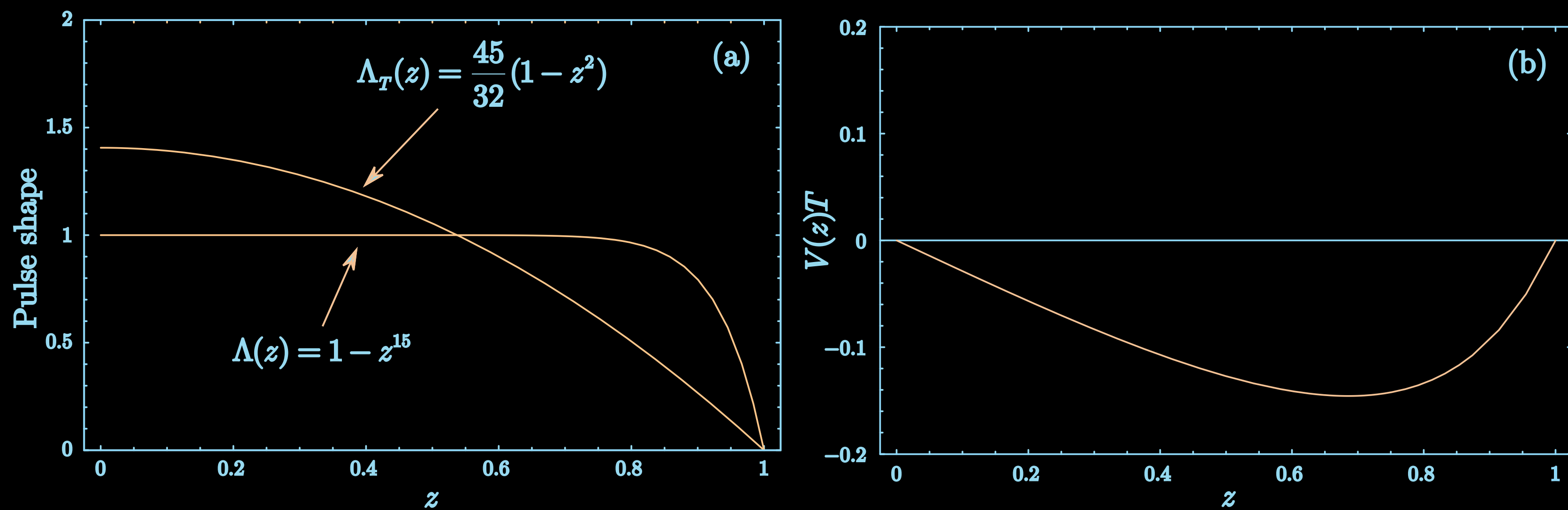

PPPL

Example 2: Pulse Shaping with Compression

$$\Lambda(z) = \begin{cases} 1 - z^m \,, & 0 \le z \le 1 \,, \\ 0 \,, & 1 < z \,, \\ \Lambda(-z) \,, & z < 0 \,, \end{cases}$$

$$\Lambda_T(z) = \begin{cases} [1 - (\alpha z)^n] \dfrac{\alpha m (n+1)}{n(m+1)} \,, & 0 \le z \le \dfrac{1}{\alpha} \,, \\ 0 \,, \ \dfrac{1}{\alpha} < z \,, \\ \Lambda(-z) \,, & z < 0 \,, \end{cases} .$$

⇨ The equation for U can be integrated to give

$$\left[\alpha U(\xi) - \frac{(\alpha U(\xi))^{n+1}}{n+1} \right] \frac{m(n+1)}{n(m+1)} = \xi - \frac{\xi^{m+1}}{m+1} \,,$$

$$\alpha U(\xi = 1) = 1, \text{ and } V(\xi = 1) = \frac{(1/\alpha - 1)}{T} \,.$$

Example: Pulse Shaping with Compression

- For the case of a beam being shaped but not compressed, $\alpha = 1$ and $V(\xi = 1) = 0$. When $\alpha > 1$, the beam is simultaneously being shaped and compressed, and $V(\xi = 1) < 0$.

- Initial pulse shape $\Lambda(z) = 1 - z^{15}$ and final pulse shape $\Lambda_T(z) = (135/32)(1 - 9z^2)$ are plotted in (a). The initial velocity $V(z)$ is plotted in (b).

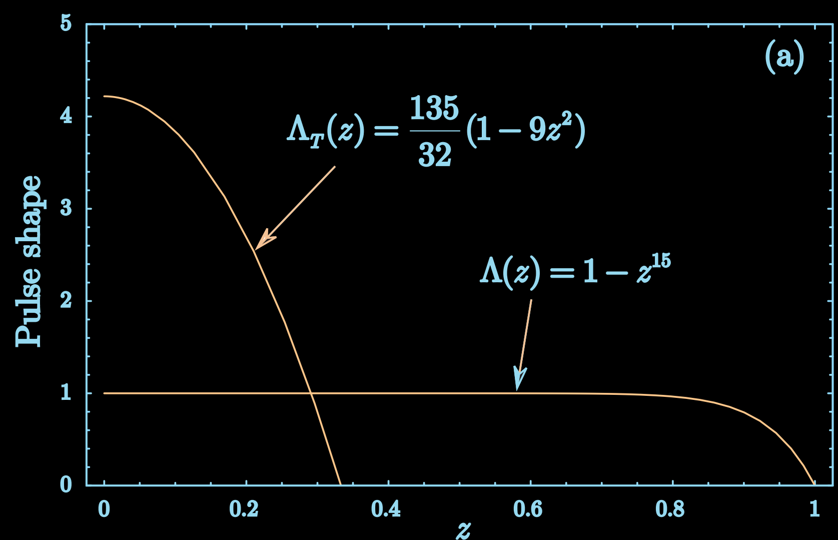

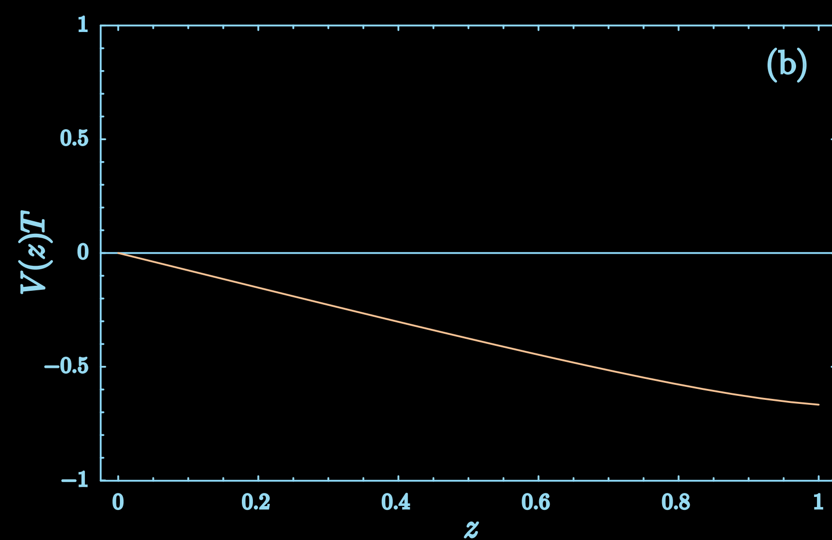

1st Order Space-Charge Correction

⇨ We now carry out the analysis to $O(\overline{K}_l)$. Let

$$\begin{aligned}\lambda(t,z) &= \lambda_0(t,z)+\lambda_1(t,z)\,,\\ v_z(t,z) &= v_{z0}(t,z)+v_{z1}(t,z)\,.\end{aligned}$$

⇨ To $O(\overline{K}_l)$,

$$\begin{aligned}\left(\frac{d}{dt}\right)_0\lambda_1 &= \frac{\partial\lambda_1}{\partial t}+v_{z0}\frac{\partial\lambda_1}{\partial z}=-\lambda_1\frac{\partial v_{z0}}{\partial z}-\frac{\partial}{\partial z}(\lambda_0 v_{z1})\,,\\ \left(\frac{d}{dt}\right)_0 v_{z1} &= \frac{\partial v_{z1}}{\partial t}+v_{z0}\frac{\partial v_{z1}}{\partial z}=-v_{z1}\frac{\partial v_{z0}}{\partial z}-\overline{K}_l\frac{\partial\lambda_0}{\partial z}\,.\end{aligned}$$

⇨ Using the method of variational coefficients, the solution is found to be

$$v_{z1}=\frac{1}{1+V_0'(\xi)t}\left\{V_1(\xi)-\overline{K}_l\frac{\partial}{\partial\xi}\left[\frac{\Lambda_0(\xi)}{V_0'(\xi)}\ln[1+V_0'(\xi)t]\right]\right\}\,.$$

1st Order Space-Charge Correction

⇨ By the same procedure,

$$\lambda_1 = \frac{\Lambda_1(\xi)}{1+V_0'(\xi)t} - \frac{1}{1+V_0'(\xi)t}\frac{\partial}{\partial\xi}\left\{\frac{\Lambda_0(\xi)V_1(\xi)t}{1+V_0'(\xi)t}\right.$$
$$- \overline{K}_l\Lambda_0(\xi)\frac{\partial}{\partial\xi}\left[\frac{\Lambda_0(\xi)}{V_0'(\xi)}\right]\frac{V_0'(\xi)t - \ln[1+V_0'(\xi)t]}{[1+V_0'(\xi)t]^2}$$
$$\left. - \overline{K}_l\frac{\Lambda_0^2(\xi)}{V_0'(\xi)}V_0''(\xi)\frac{t^2}{[1+V_0'(\xi)t]^2}\right\}.$$

⇨ At time $t = T$, we obtain

$$\boxed{\Lambda_T(z) = \lambda_0(t=T,z) + \lambda_1(t=T,z).}$$

Since $\Lambda_T(z)$ and $\Lambda(z)$ are prescribed in the pulse shaping problem, we take $\Lambda_{T1}(z) = 0$ and $\Lambda_1(z) = 0$. This results in

$$V_1(\xi) = \overline{K}_l\frac{\partial}{\partial\xi}\left[\frac{\Lambda_0(\xi)}{V_0'(\xi)}\right]\frac{V_0'(\xi) - \ln[1+V_0'(\xi)T]/T}{1+V_0'(\xi)T}$$
$$+ \overline{K}_l\frac{\Lambda_0(\xi)}{V_0'(\xi)}V_0''(\xi)\frac{T}{1+V_0'(\xi)T} + c'.$$

PPPL

Correction for Deviation from the Symmetry

- To focus entire beam pulse onto the same focal, the self-similar symmetry condition need to be satisfied.
- Self-similar drift compression scheme satisfies the symmetry condition for the line density.
- It is difficult to guarantee the symmetry condition for the transverse emittance due to the complex dynamical behavior.
  - Longitudinal compression
  - Non-periodic transverse focusing lattice and final focus magnets.
- However, in most heavy ion fusion systems, the transverse emittance is small.
- The deviation from the self-similar symmetry condition due to the transverse emittance can be treated as a perturbation.
- Deliberately impose another perturbation to the system to cancel out the perturbation due to the un-symmetric transverse emittance.

Correction for Deviation from the Symmetry

- Demonstrate this technique using the parabolic longitudinal drift compression scheme for a typical un-neutralized heavy ion fusion beam.

- The perturbation introduced to cancel out the un-symmetric emittance effect will be four time-dependent magnets.

- First, a drift compression and final focus lattice is designed for the central slice $(Z = 0)$, and then four quadrupole magnets at the beginning of the drift compression are replaced by four time-dependent magnets whose strength varies around the design value for the central slice.

- The time-dependent magnets essentially provide a slightly different focusing lattice for the different slices.

- Transverse envelope equations for every slice in a bunched beam,

$$\boxed{\begin{aligned} \frac{\partial^2 a(s,Z)}{\partial s^2} + \kappa_q a(s,Z) - \frac{2K(s,Z)}{a(s,Z)+b(s,Z)} - \frac{\varepsilon_x^2(s,Z)}{a(s,Z)^3} &= 0, \\ \frac{\partial^2 b(s,Z)}{\partial s^2} - \kappa_q b(s,Z) - \frac{2K(s,Z)}{a(s,Z)+b(s,Z)} - \frac{\varepsilon_y^2(s,Z)}{b(s,Z)^3} &= 0, \end{aligned}}$$

Correction for Deviation from the Symmetry

- ⇨ $K(s,z)$ is non-periodic due to the longitudinal compression.
- ⇨ κ_q need to be non-periodic to reduce the expansion of the beam radius.
- ⇨ Since the quadrupole lattice is not periodic, the concept of a “matched” beam is not well defined.
- ⇨ However, if the the non-periodicity is small, that is, if the quadrupole lattice changes slowly along the beam path, we can seek an “adiabatically”-matched beam which, by definition, is locally matched everywhere.

Non-periodic Lattice Design for Central Slice

- Goal:
  - Constant vacuum phase advance $\sigma_v = \pi/5 \longrightarrow \eta B' L^2 = const.$
  - Length $z_b \longrightarrow \times\frac{1}{21.8}$. Perveance $K \longrightarrow \times 21.8$.
  - Beam radius $a \longrightarrow \times 2.33$.
  - Half lattice period $L \longrightarrow \times\frac{1}{2}$.
  - Filling factor $\eta \longrightarrow \times 4$. $\eta B' \longrightarrow \times 4$.
- How do $K,\ L, \eta,\ B',\ a$, and b depend on s?
  - $K(s)$ is given by the longitudinal dynamics.
  - $L(s), \eta(s)$, and $B'(s)$ are determined by requirements such as constant vacuum phase advance.
  - $a(s)$ and $b(s)$ are determined by the transverse envelope equations.

Non-periodic Lattice Design for Central Slice

- A lattice which keeps both the vacuum phase advance and depressed phase advance constant is less likely to induce beam mismatch.
- Vacuum phase advance σ_v and depressed phase advance σ are given by

$$2(1-\cos\sigma_v) = (1-\frac{2\eta}{3})\eta^2\left(\frac{B'}{[B\rho]}\right)^2 L^4,$$

$$\sigma^2 = 2(1-\cos\sigma_v) - K\left(\frac{2L}{\langle a\rangle}\right)^2 .$$

- Assuming $\eta \ll 1$, we obtain

$$\boxed{\eta^2(\frac{B'}{[B\rho]})^2 L^4 = const.,\ \ K(\frac{2L}{\langle a\rangle})^2 = const.,}$$

for constant vacuum phase advance and constant depressed phase advance.

- It is under-determined. As one possible choice, let

$$L = L_0\exp(-\ln 2\frac{s}{s_f}), \qquad \eta = \eta_0\exp(2\ln 2\frac{s}{s_f}), \qquad B' = const.$$

Non-periodic Lattice Design for Central Slice

- Let the lattice lengths are $L_0,\ L_1,\ \ldots,\ L_N = L_f$,

$$L_1 = L_0 \exp(-\ln 2 \frac{2L_0}{s_f}),$$

$$L_2 = L_0 \exp(-\ln 2 \frac{2(L_0 + L_1)}{s_f}),$$

$$\ldots\ldots$$

$$L_i = L_0 \exp(-\ln 2 \frac{2\sum_0^{i-1} L_i}{s_f}),$$

$$2(L_1 + L_2 + \ldots + L_N) = S_f.$$

- For $L_f = 3.36\text{m}$, $L_0 = 6.72\text{m}$, and $s_f = 421.5\text{m}$, calculation gives $N = 45$.
- For an adiabatically-matched solution,
  - The envelope is locally matched and contains no oscillations other than the local envelope oscillations.
  - On the global scale, the beam radius increases monotonically.

Final Focus Magnets for Central Slice

- Four final focus quadrupole magnets assure that the envelope converge in both directions at the exit of the last focusing magnet.

- Then the beam enters the neutralization chamber where the space-charge force is neutralized, and is focused onto a focal point at

$$\boxed{z_{fol} = -\left.\frac{a}{\partial a/\partial s}\right|_{s=s_{ff}} = -\left.\frac{b}{\partial b/\partial s}\right|_{s=s_{ff}} ,}$$

- The transverse spot size is determined by the emittance and incident angle at $s = s_{ff}$,

$$\boxed{a_{fol} = \left.\frac{\varepsilon_x}{\partial a/\partial s}\right|_{s=s_{ff}} , \; b_{fol} = \left.\frac{\varepsilon_y}{\partial b/\partial s}\right|_{s=s_{ff}} .}$$

- For the central slice at $z = 0$, we obtain $z_{fol} = 5.276\,\mathrm{m}$, and $a_{fol} = b_{fol} = 1.22\,\mathrm{mm}$.

Transverse Dynamics for Central Slice

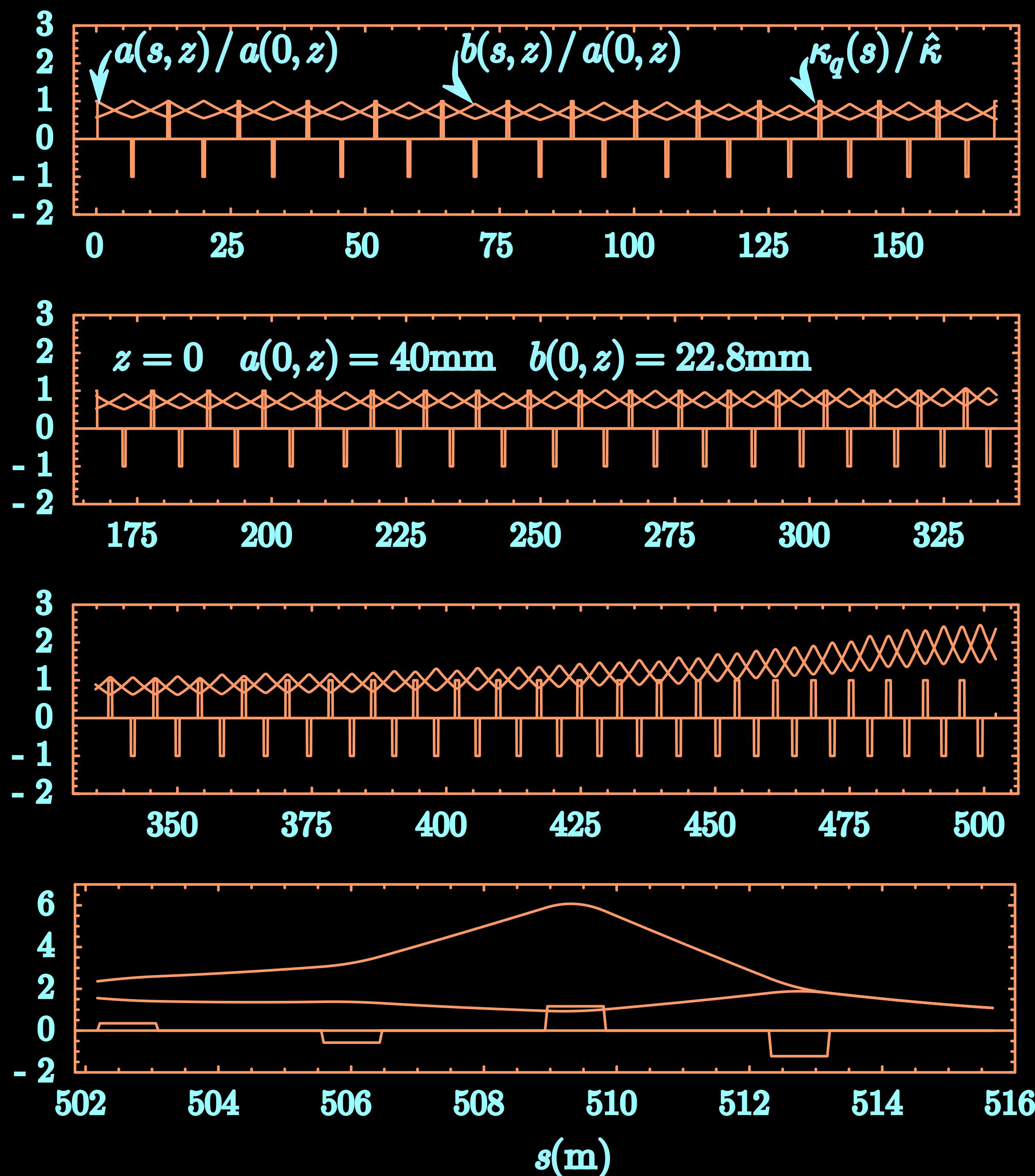

Time-Dependent Lattice for Entire Pulse

⇨ Other slices ($Z = z/z_b \neq 0$) should be focused onto the same focal point

$$\boxed{z_{fol} = 5\,\mathrm{m}, \quad a_{fol} \approx b_{fol} \lesssim 1.2\,\mathrm{mm}\,.}$$

⇨ For the $\lambda(s,z) = \lambda_b(s)[1 - z^2/z_b^2(s)]$, the self-similar symmetry condition implies that the solution for all of the slices can be scaled down from that of the central slice:

$$\boxed{\begin{pmatrix} a(s,z) \\ b(s,z) \\ \partial a(s,z)/\partial s \\ \partial b(s,z)/\partial s \end{pmatrix} = \sqrt{1 - z^2/z_b^2(s)} \begin{pmatrix} a(s,0) \\ b(s,0) \\ \partial a(s,0)/\partial s \\ \partial b(s,0)/\partial s \end{pmatrix},}$$

if the emittance is

- negligibly small or
- scales with the perveance according to $(\varepsilon_x, \varepsilon_y) \propto 1 - z^2/z_b^2(s)$.

Time-Dependent Lattice for Entire Pulse

- ⇨ However, the emittance in general is small but not negligible, and does not scale with the perveance.
- ⇨ In fact, during adiabatic drift compression, the emittance scales with the beam size, i.e., $\varepsilon_x \propto a$ and $\varepsilon_y \propto b$.
- ⇨ Self-similar symmetry condition can't be satisfied.
- ⇨ Vary the strength of four magnets in the very beginning of the drift compression for different value of z such that the self-similar symmetry holds at $s = s_{ff}$.
- ⇨ Numerically, the necessary variation of the strength of the magnets is found by a 4D root-searching algorithm.
- ⇨ A small perturbation in the strength of the magnets introduces a small envelope mismatch in such a way that the self-similar symmetry is satisfied at $s = s_{ff}$.

Envelope dynamics for the $z/z_b(s) = 0.968$.

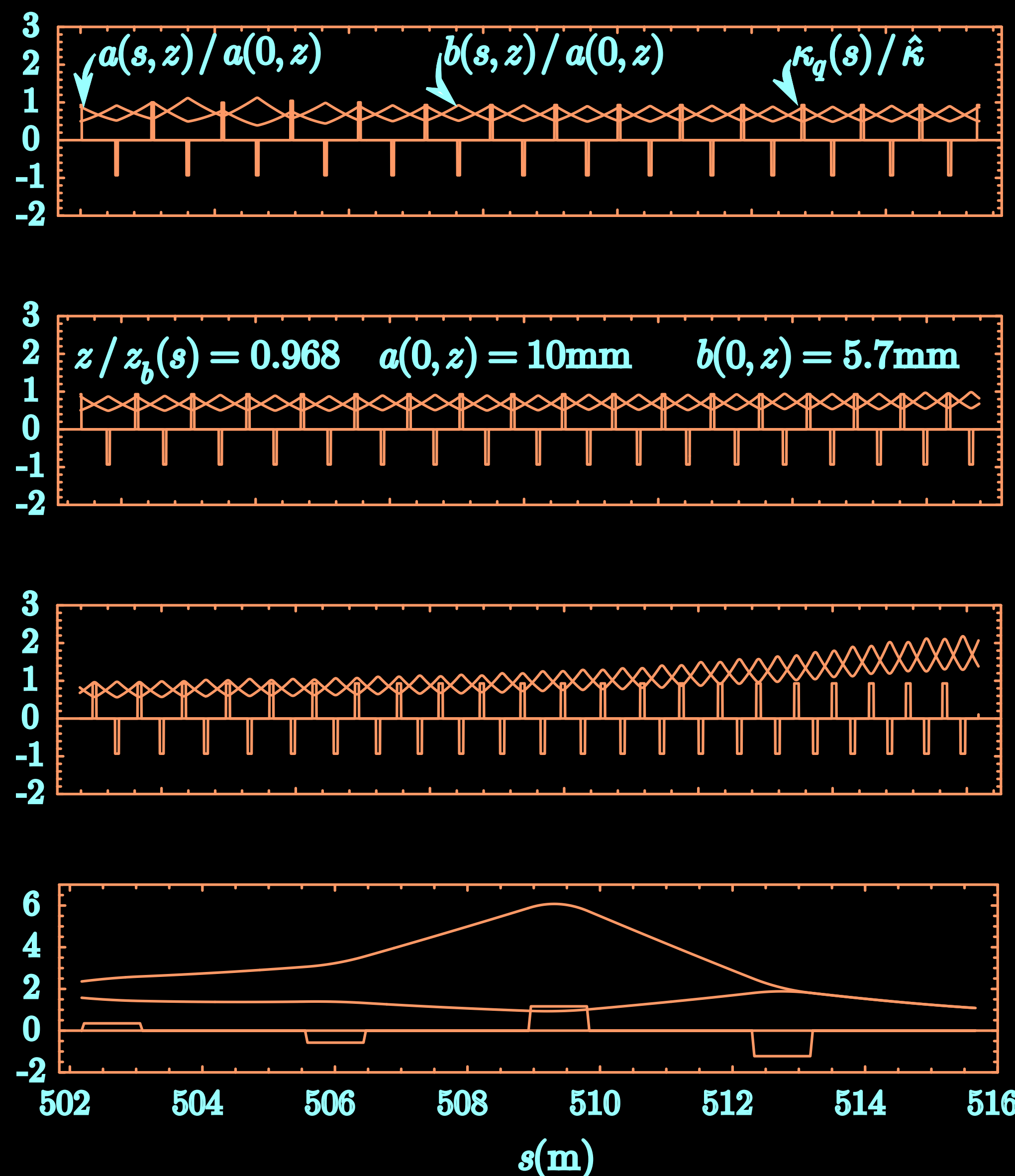

Time-Dependent Lattice for Entire Pulse

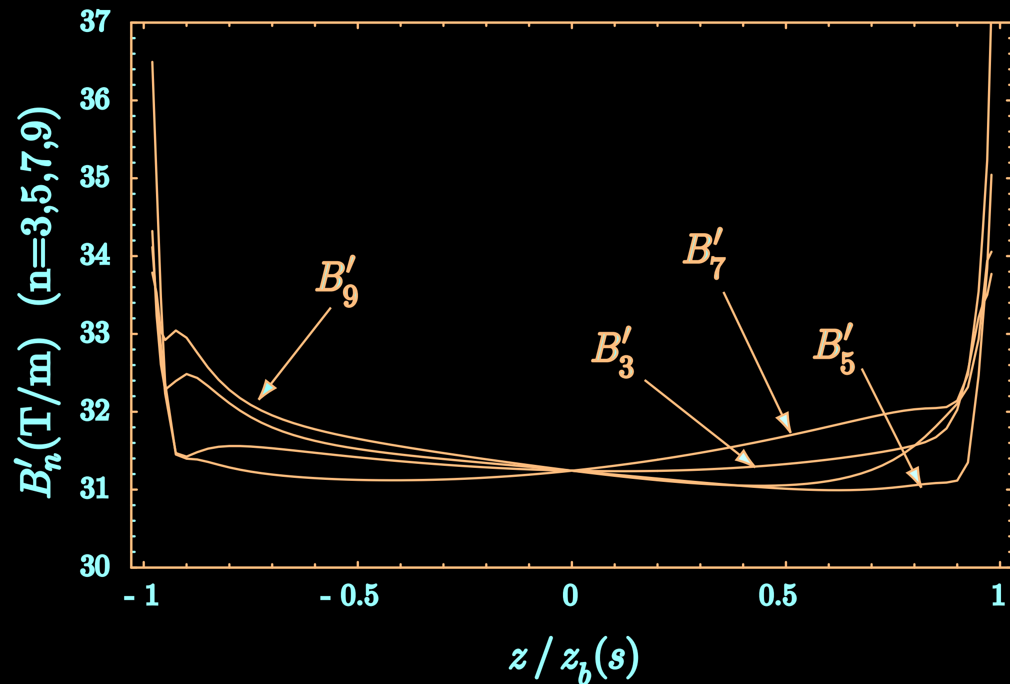

Figure 1: Strengths of the 3rd, 5th, 7th, and 9th magnets as functions of $z/z_b(s)$.

Conclusion

- Two of the most important requirements of the drift compression and final focus systems were considered.
  - A large compression ratio needs to be achieved.
  - The entire beam pulse needs to be focused onto the same focal spot at the target.
- It is necessary to use a self-similar drift compression scheme.
  - For un-neutralized beams, the Lie symmetry group analysis was applied to the warm-fluid model to systematically derive the self-similar drift compression solutions.
  - For neutralized beams, the 1D Vlasov equation was solved explicitly and families of self-similar drift compression solutions were constructed.
- A non-periodic lattice has been designed so that it is possible to actively control the transverse size of the beam.

Conclusion

- To compensate for the deviation from the self-similar symmetry condition, four time-dependent magnets were introduced in the upstream such that the entire beam pulse can be focused onto the the same focal spot.

- The self-similar longitudinal drift compression scheme, combined with the non-periodic, time-dependent lattice design, provide the essential elements of a leading-order drift compression method.

- The next-step investigation will be focused on second-order effects, such as emittance growth during drift compression, and the two-way coupling between the longitudinal and transverse dynamics.